

### Application of Chiral Mixed Phosphorus/Sulfur Ligands to Enantioselective Rhodium-Catalyzed Dehydroamino Acid Hydrogenation and Ketone Hydrosilylation Processes

David A. Evans,\* Forrest E. Michael, Jason S. Tedrow, and Kevin R. Campos

Contribution from the Department of Chemistry and Chemical Biology, Harvard University, Cambridge, Massachusetts 02138

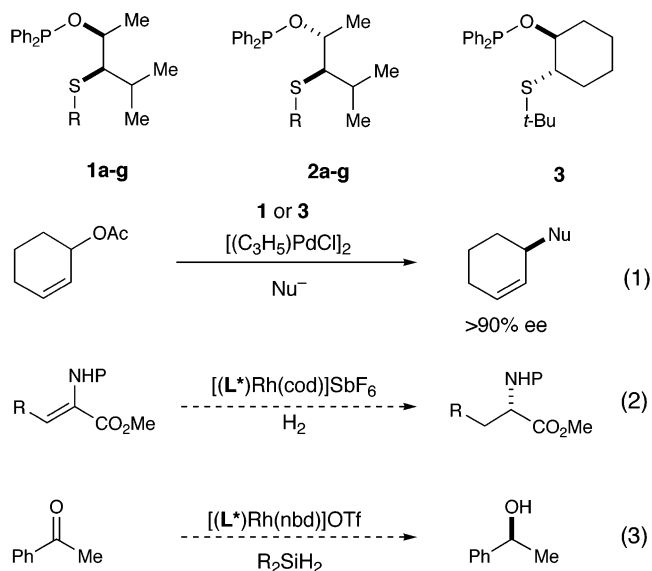
Received December 3, 2001; Revised Manuscript Received December 18, 2002; E-mail: evans@chemistry.harvard.edu

**Abstract:** Chiral mixed phosphorus/sulfur ligands **1–3** have been shown to be effective in enantioselective Rh-catalyzed dehydroamino acid hydrogenation and ketone hydrosilylation reactions (eqs 1, 2). After assaying the influence of the substituents at sulfur, the substituents on the ligand backbone, the relative stereochemistry within the ligand backbone, and the substituents at phosphorus, ligands **2c** (R = 3,5-dimethylphenyl) and **3** were found to be optimal in the Rh-catalyzed hydrogenation of a variety of  $\alpha$ -acylaminoacrylates in high enantioselectivity (89–97% ee). A similar optimization of the catalyst for the Rh-catalyzed hydrosilylation of ketones showed that ligand **3** afforded the highest enantioselectivities for a wide variety of aryl alkyl and dialkyl ketones (up to 99% ee). A model for asymmetric induction in the hydrogenation reaction is discussed in the context of existing models, based on the absolute stereochemistry of the products and the X-ray crystal structures of catalyst precursors and intermediates.

#### Introduction

**Objectives.** We recently reported a new family of chiral P/S ligands and examined their utility in enantioselective Pd-catalyzed allylic alkylation and amination of acyclic and cyclic substrates (eq 1).<sup>1</sup> In the present study, we have now evaluated this same family of chiral ligands in Rh-catalyzed hydrogenation and hydrosilylation processes (eqs 2, 3). The Pd and Rh complexes employed in these processes are structurally homologous square planar d<sup>8</sup> metals complexed by a common ligand family. Accordingly, the origins of stereoinduction may be inferred from the interplay of the trans influence and metal-induced sulfur chirality.

The asymmetric Rh-catalyzed hydrogenation of enamides has been extensively studied, and a variety of chiral bisphosphines are very effective ligands for this transformation.<sup>2</sup> However, few examples of this process have been reported with mixed donor ligands, all of which are plagued by low reactivity or selectivity or both.<sup>3</sup> Furthermore, there is a large body of mechanistic data<sup>4</sup> that could be useful for reaction optimization and mechanistic study. In contrast to hydrogenation, a large



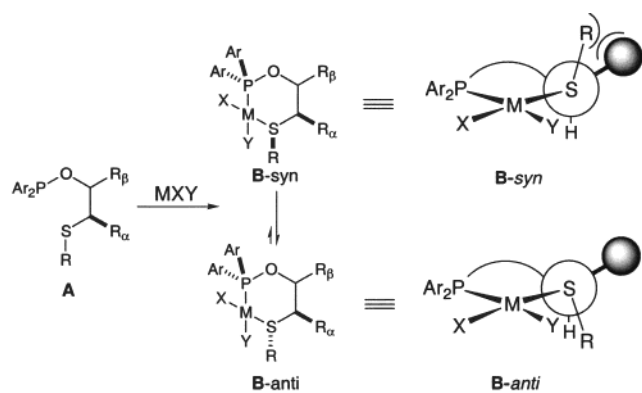
number of catalysts have been assayed in the Rh-catalyzed hydrosilylation of ketones, many of them involving mixed donor ligands, but few have displayed wide substrate generality, especially regarding the reduction of dialkyl ketones.<sup>5</sup> We felt that an investigation of these mixed phosphorus/sulfur ligands in the indicated Rh-catalyzed transformations provided an excellent opportunity to evaluate the generality of these ligands in asymmetric catalysis.

**Ligand Design Attributes.** The identification and discovery of new methods for transferring chirality between catalysts and their substrates is of primary importance in the discovery of new enantioselective processes. The crucial stereodefining

- (1) Evans, D. A.; Campos, K. R.; Tedrow, J. S.; Michael, F. E.; Gagne, M. R. *J. Am. Chem. Soc.* **2000**, *122*, 7905–7920.  
 (2) (a) For a review, see: Noyori, R.; Takaya, H.; Ohta, T. *Catalytic Asymmetric Synthesis*; Ojima, I., Ed.; VCH Publishers: Weinheim, 1993; pp 1–39. (b) Burk, M. J.; Feaster, J. E.; Nugent, W. A.; Harlow, R. L. *J. Am. Chem. Soc.* **1993**, *115*, 10125–10138. (c) Burk, M. *Acc. Chem. Res.* **2000**, *33*, 363–372. (d) Zhu, G.; Cao, P.; Jiang, Q.; Zhang, X. *J. Am. Chem. Soc.* **1997**, *119*, 1799–1800. (e) Zhu, G.; Zhang, X. *J. Org. Chem.* **1998**, *63*, 3133–3136.  
 (3) (a) Hauptman, E.; Shapiro, R.; Marshall, W. *Organometallics* **1998**, *17*, 4976–4982. (b) Berger, H.; Nesper, R.; Pregosin, P.; Ruegger, H.; Worle, M. *Helv. Chim. Acta* **1993**, *76*, 1520–1538. (c) Yamada, I.; Ohkouchi, M.; Yamaguchi, M.; Yamagishi, T. *J. Chem. Soc., Perkin Trans. 1* **1997**, 1869–1873.  
 (4) Feldgus, S.; Landis, C. R. *J. Am. Chem. Soc.* **2000**, *122*, 12714–12727 and references therein. Also see ref 2.

elements for the mixed phosphorus/sulfur ligands are the selective formation of a stereogenic center at sulfur upon coordination to a metal center and the use of electronic effects such as the trans influence<sup>6</sup> to control the relative stability and reactivity of the potential diastereomeric intermediates. In the case of the allylic alkylation reaction,<sup>1</sup> the sulfur-induced asymmetry was used to control the orientation of the allylpalladium complex, while the trans influence determined the regiochemistry of nucleophilic attack, resulting in a highly enantioselective process.

Because metal-coordinated thioethers have a low inversion barrier, an effective means of controlling the configuration at sulfur must be designed into the ligand scaffold. Ligand class **A** achieves this control by positioning a large gearing substituent adjacent to the sulfur donor ( $R_\alpha$ ), forcing the sulfur substituent into an anti orientation to avoid unfavorable steric interactions. Addition of a substituent in the beta position ( $R_\beta$ ) helps to increase the effective size of the alpha substituent and, by proper choice of relative stereochemistry, to control the conformation of the chelate ring. In this manner, formation and control of a stereogenic center that is directly attached to the metal increases the likelihood of effective stereochemical communication between the ligand and the reactive site. Furthermore, the difference in trans influence between the phosphorus and sulfur donors electronically differentiates the two binding sites, making the ligand trans to the stronger phosphorus donor, Y, more labile. This architecture places the more reactive site adjacent to the stereogenic sulfur center, further maximizing its stereochemical impact.



A modular approach to the synthesis of ligand class **A** allows the substituents at phosphorus (Ar), sulfur (R), and on the backbone ( $R_\alpha$ ,  $R_\beta$ ) to be varied independently. The effect of each of these substituents on ligand performance may then be rapidly assayed. Ligands **1–3** were shown to be optimal for

the asymmetric allylation reaction, and therefore constituted a suitable starting point in the search for a viable Rh-catalyzed process.

In the following sections, the degree of structural similarity between Pd and Rh complexes of ligands **1–3** is investigated. Then, a set of structurally diverse phosphorus/sulfur (P/S) ligands is evaluated in the Rh-catalyzed hydrogenation of  $\alpha$ -acylaminoacrylates and the hydrosilylation of ketones. After optimization of catalyst structure and conditions, the breadth of substrate tolerance is investigated. For the hydrogenation reaction, a stereochemical model is proposed, and the X-ray crystal structure of an important intermediate is provided to support that model.

### Comparison of Rhodium and Palladium Chelate Geometries

Our initial investigations into the Rh-catalyzed transformations with mixed P/S ligands began with the development of a well-defined catalyst precursor. Treatment of  $[(\text{cod})_2\text{Rh}]\text{SbF}_6$  with 1 equiv of **2g** afforded the cationic complex  $[(\text{2g})\text{Rh}(\text{cod})]\text{SbF}_6$  (**4a**). Suitable crystals of this complex were obtained and subjected to X-ray crystallographic analysis (Figure 1).<sup>7</sup> A comparison of the crystal structure of **4a** to that obtained for  $(\text{2g})\text{PdCl}_2$  (**5a**)<sup>1</sup> reveals that the chelate geometries are almost identical, including the twist-boat conformation of the chelate ring and the effective gearing of the sulfur substituent by the isopropyl group.

A comparison of the X-ray crystal structures of Rh complex **4b**<sup>8</sup> and Pd complex **5b**<sup>1</sup> of syn substituted ligand **1g** also reveals a high level of homology (Figure 2). Notably, instead of the twist-boat conformation observed for complexes **4a** and **5a** and **4b** and **5b** both prefer a pseudochair conformation to avoid positioning the  $\beta$ -methyl group in the unfavorable flagpole position. The sulfur substituent, however, remains disposed in a pseudoaxial conformation. While it seems likely that this predilection for axial disposition of the pendant sulfur substituent<sup>9</sup> is to avoid unfavorable steric interactions between this group and the square planar metal center, an electronic effect cannot be ruled out. This pseudoaxial orientation is important because it fixes the orientation of the *P*-phenyl substituents, and the documented importance of *P*-phenyl edge-on/face-on relationships for high enantioselectivities in the Rh-catalyzed hydrogenation of acetamidocinnamates<sup>10</sup> prompted the investigation of this transformation with this ligand class.

### Hydrogenation of Acetamidoacrylates

**Catalyst Optimization.** Complex **4a** (Figure 1) was an effective catalyst precursor for the hydrogenation of (*Z*)-methyl acetamidocinnamate (**6a**). Under 7.8 atm  $\text{H}_2$  at 55 °C in THF, catalyst **4a** effectively reduced **6a** to the desired *N*-protected

- (5) (a) For hydrosilylation catalysts with high substrate generality, see: Sawamura, M.; Kuwano, R.; Ito, Y. *Angew. Chem., Int. Ed. Engl.* **1994**, *33*, 111–113. (b) For early work on hydrosilylation with mixed donor ligands, see: Brunner, H.; Reipl, G.; Weitzer, H. *Angew. Chem., Int. Ed. Engl.* **1983**, *22*, 331–332. Brunner, H.; Becker, R.; Reipl, G. *Organometallics* **1984**, *3*, 1354–1359. (c) For reviews of asymmetric hydrosilylation, see: Nishiyama, H.; Itoh, K. *Catalytic Asymmetric Synthesis*, 2nd ed.; Ojima, I., Ed.; VCH Publishers: Weinheim, 2000, pp 111–143. *Catalytic Asymmetric Synthesis*; Ojima, I., Ed.; VCH Publisher: Weinheim, 1993; Chapter 6. Brunner, H. *Transition Metals in Organic Synthesis*; Beller, M., Ed.; Wiley-VCH: Weinheim, 1998; pp 131–140. (d) Further advances have also been made in this area with titanocene catalysts, see: Carter, M. B.; Schiott, B.; Gutierrez, A.; Buchwald, S. L. *J. Am. Chem. Soc.* **1994**, *116*, 11667–11670. Yun, J.; Buchwald, S. L. *J. Am. Chem. Soc.* **1999**, *121*, 5640–5644.
- (6) (a) Appleton, T. G.; Clark, H. C.; Manzer, L. E. *Coord. Chem. Rev.* **1973**, *10*, 335–422. (b) Murray, S.; Hartley, F. *Chem. Rev.* **1981**, *81*, 365–414.

- (7) Crystals of **4a** ( $\text{C}_{30}\text{H}_{43}\text{F}_6\text{ORhSbPS}$ ) were grown by slow diffusion of  $\text{Et}_2\text{O}$  into a solution of **4a** in  $\text{CH}_2\text{Cl}_2$  to yield orange needles. The compound crystallizes in the monoclinic crystal system, space group  $P2_1$ ;  $a = 9.3865(7)$  Å,  $b = 15.6932(12)$  Å,  $c = 11.6319(9)$  Å,  $\alpha = \gamma = 90^\circ$ ,  $\beta = 98.987(2)^\circ$ ;  $V = 1692.4(2)$  Å<sup>3</sup>;  $Z = 2$ ;  $R = 0.0695$ ,  $\text{Goof} = 1.149$ .
- (8) Crystals of **4b** ( $\text{C}_{30}\text{H}_{43}\text{F}_6\text{ORhSbPS}$ ) were grown by slow diffusion of  $\text{Et}_2\text{O}$  into a solution of **4b** in  $\text{CH}_2\text{Cl}_2$  to yield orange needles. The compound crystallizes in the orthorhombic crystal system, space group  $P2_12_12_1$ ;  $a = 10.9184(10)$  Å,  $b = 16.260(3)$  Å,  $c = 18.966(2)$  Å,  $\alpha = \beta = \gamma = 90^\circ$ ;  $V = 3367.1(7)$  Å<sup>3</sup>;  $Z = 4$ ;  $R = 0.0276$ ,  $\text{Goof} = 1.022$ .
- (9) The tendency for sulfur substituents in palladium P/S chelate rings to adopt a pseudoaxial orientation has been previously noted. See: Barbaro, P.; Currao, A.; Herrmann, J.; Nesper, R.; Pregosin, P.; Salzmann, R. *Organometallics* **1996**, *15*, 1879–1888.
- (10) Brown, J.; Evans, P. *Tetrahedron* **1988**, *44*, 4905–4916

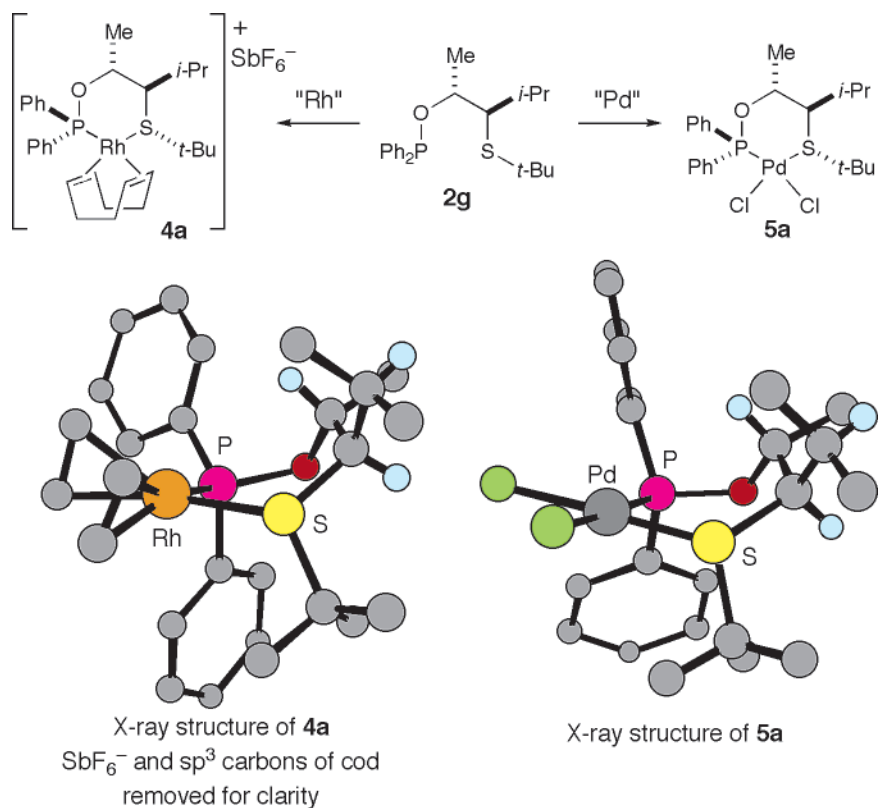


**Figure 1.** A comparison of the Rh and Pd complexes of **2g**.

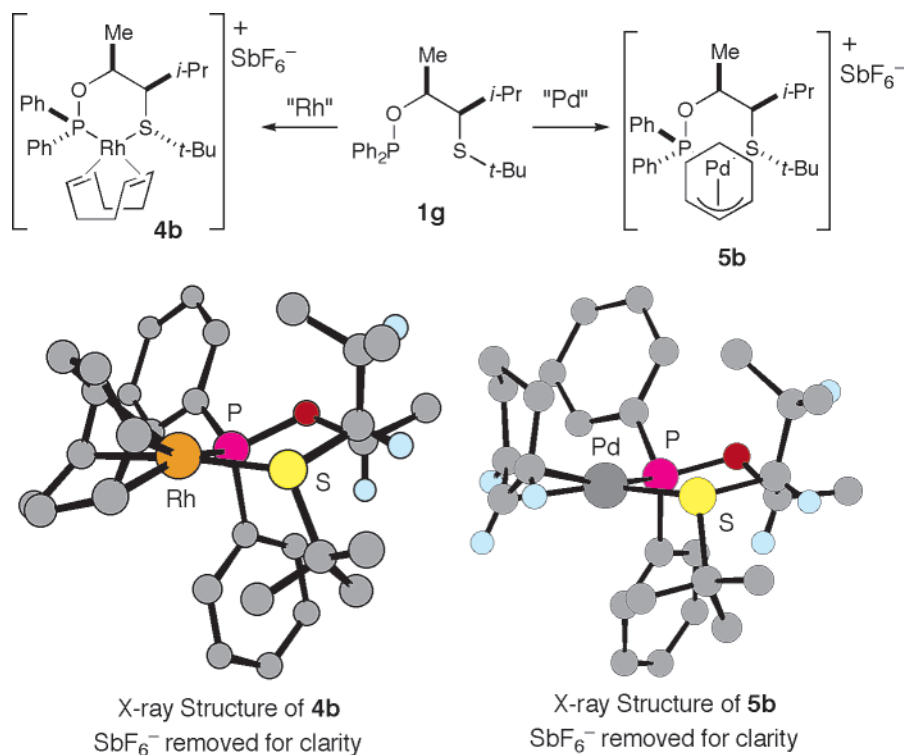


**Figure 2.** A comparison of the Rh and Pd complexes of **1g**.

$\alpha$ -aminoester **7a** in 76% ee. The same reaction at room temperature afforded the product in slightly lower selectivity and low conversion. These conditions, however, (rt, 7.8 atm H<sub>2</sub>) turned out to give the highest levels of enantioselectivity for ligands **1** and **2**, slightly better than the results at atmospheric

pressure.<sup>11</sup> It is interesting to note that this is in direct contrast to many other Rh-catalyzed hydrogenation processes where increasing the hydrogen pressure has a detrimental effect on

(11) For ligand **2e**, 1 atm H<sub>2</sub> gave 87% ee, while 7.8 atm H<sub>2</sub> gave 90% ee.

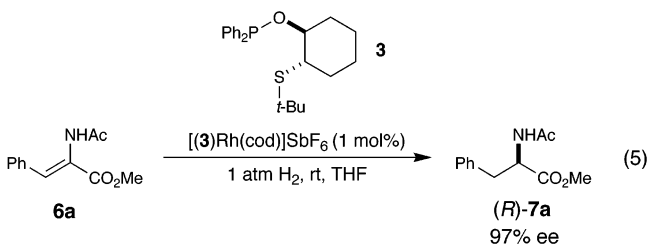
**Table 1.** Hydrogenation of (*Z*)-Methyl Acetamidocinnamate with Mixed Phosphorus/Sulfur Ligands (eq 4)<sup>a</sup>

R	L*, % ee <sup>b,c</sup>	L*, % ee <sup>b,c</sup>
Ph	<b>1a</b> , 84	<b>2a</b> , 95
4-MeOPh	<b>1b</b> , 78	<b>2b</b> , 82
3,5-Me <sub>2</sub> Ph	<b>1c</b> , 81	<b>2c</b> , 97
1-Nap	<b>1d</b> , 87	<b>2d</b> , 93
Bn	<b>1e</b> , 82	<b>2e</b> , 90
Cy	<b>1f</b> , 84	<b>2f</b> , NR
<i>t</i> -Bu	<b>1g</b> , 82	<b>2g</b> , 68 (20% conv)

<sup>a</sup> All reactions proceeded to complete conversion, except where noted otherwise. <sup>b</sup> Determined by chiral HPLC (Chiralcel OJ). <sup>c</sup> Absolute stereochemistry determined by comparison of optical rotation to literature values.

enantioselectivity.<sup>12</sup> A variety of acyclic P/S ligands were screened under these hydrogenation conditions and, as was seen in the Pd-catalyzed allylic substitution, ligand architecture **2** generally afforded superior enantioselectivities to **1** (Table 1). In this case, the notable exceptions were **2f** and **2g** where the larger alkyl substituents on sulfur appear to adversely effect the reactivity and selectivity.

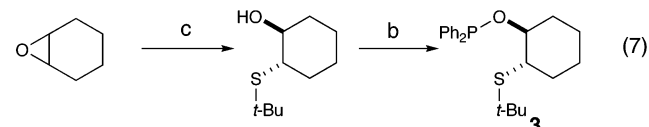
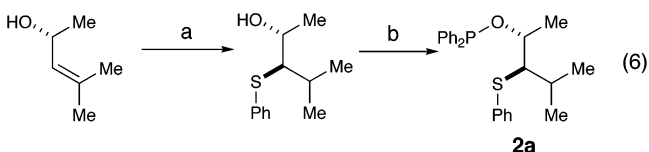
In contrast to Pd-catalyzed allylic substitutions, where bulky *S*-alkyl substituents proved optimal, the enantioselectivities in the Rh-catalyzed hydrogenation were superior with smaller sulfur substituents. In fact, ligands bearing *S*-aryl substituents (e.g., **2a**, **2c**, **2d**), generally afforded higher enantioselectivities than their *S*-alkyl counterparts. The optimal ligand was found to be **2c**, with a 3,5-dimethylphenyl substituent at sulfur, which afforded hydrogenated product **7a** in 97% ee.



Although *S*-*tert*-butyl substituents in the acyclic ligand scaffolds **1** and **2** afforded only moderate enantioselectivities in the hydrogenation of (*Z*)-methyl acetamidocinnamate, structural analogue **3** was highly effective, affording hydrogenated product in 97% ee (eq 5). In contrast to ligands **1** and **2**, hydrogenation reactions involving ligand **3** gave slightly better results at 1 atm H<sub>2</sub>. The absolute sense of induction using this ligand (*R*) is the opposite of that obtained using ligands **1** and **2** because the stereocenter alpha to the sulfur donor is inverted.

The optimal ligands for the hydrogenation reaction, **2** and **3**, are both available via short synthetic routes (eqs 6, 7). For example, **2a** can be made by diastereoselective sulfenylation of a chiral allylic alcohol, followed by phosphinylation. Alternatively, **3** may be derived from the enantioselective ring

opening of cyclohexene oxide with *tert*-butanethiol,<sup>13</sup> followed by phosphinylation of the resultant alcohol. Reaction conditions



were the following: (a) PhSCl, Et<sub>2</sub>O, -78 °C, then Zn(BH<sub>4</sub>)<sub>2</sub>, -78 → 0 °C. (b) BuLi, Ph<sub>2</sub>PCl (c) *t*-BuSH, (BINOL)<sub>2</sub>GaLi.

**Scope.** The reaction conditions using ligands **2c** and **3** were effective in the hydrogenation of a variety of alkyl- and aryl-substituted α-acetamidocrylates **6a–g**, delivering the protected α-aminoesters **7a–g** in high enantioselectivity (Table 2). These

**Table 2.** Hydrogenation of Substituted Acetamidocrylates with Mixed Phosphorus/Sulfur Ligands (eq 8)<sup>a,b</sup>

R	% ee <sup>b,d</sup> ( <i>S</i> )	% ee <sup>b,e</sup> ( <i>R</i> )
Ph ( <b>7a</b> )	97	97
4-MeOPh ( <b>7b</b> )	96	98
3-BrPh ( <b>7c</b> )	94	95
4-F, 3-NO <sub>2</sub> Ph ( <b>7d</b> )	92	94
Me ( <b>7e</b> )	97	98
Et ( <b>7f</b> )	94	94
<i>i</i> -Pr ( <b>7g</b> )	89	36

<sup>a</sup> All reactions proceeded to complete conversion. <sup>b</sup> Absolute stereochemistry of the products determined by correlation of optical rotations to literature values. <sup>c</sup> Enantiomeric excess determined by chiral GC (Chiralcel L-Val). <sup>d</sup> 7.8 atm H<sub>2</sub>. <sup>e</sup> 1.0 atm H<sub>2</sub>.

reactions were complete within 18 h at room temperature. Although the reaction rate is somewhat slower than that of catalysts containing electron-rich bisphosphines, the reaction times are still reasonable. The hydrogenation of the nitrofluorophenyl-substituted cinnamate **7d** was performed on a 5-g scale, giving the phenylalanine derivative in 96% yield and 94% ee.<sup>14</sup> Cyclic ligand **3** was not as tolerant of the sterically demanding substrate **6g**, furnishing **7g** in only 36% ee. Fortunately, the two ligand systems are complementary, and hydrogenation using ligand **2c** afforded the product in 89% ee.

An important feature of these ligands is their tolerance of a wide variety of amine protecting groups. The nature of the *N*-protecting group has little effect on the selectivity of the reaction (Table 3). Both (*E*) and (*Z*) geometries of olefin **8b** are hydrogenated in 94% ee (both affording the *S* configuration)

(13) Iida, T.; Yamamoto, N.; Sasai, H.; Shibasaki, M. *J. Am. Chem. Soc.* **1997**, *119*, 2801–2803.

(14) This hydrogenation was used in a synthesis of teicoplanin in our laboratory. Evans, D. A.; Katz, J. L.; Peterson, G. S.; Hintermann, T. *J. Am. Chem. Soc.* **2001**, *123*, 12411–12413.

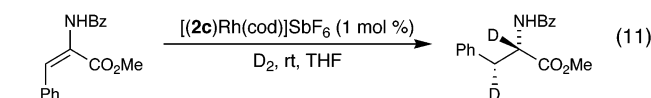
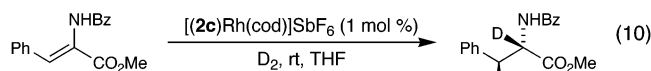
(12) Landis, C.; Halpern, J. *J. Am. Chem. Soc.* **1987**, *109*, 1746–1754.

**Table 3.** Asymmetric Hydrogenation of *N*-Acylaminocinnamates with Mixed Phosphorus/Sulfur Ligands (eq 9)<sup>a,b</sup>

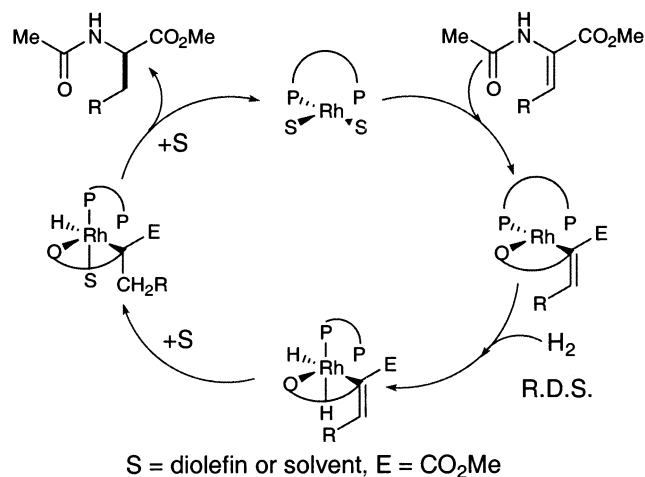
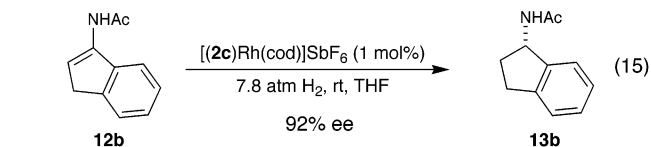
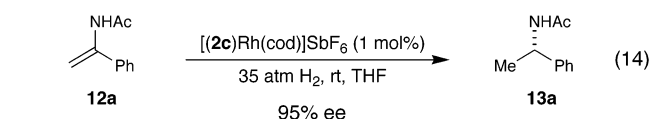
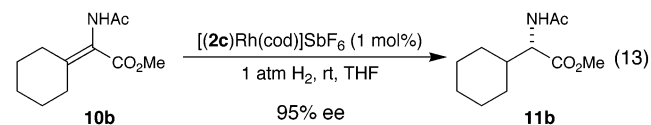
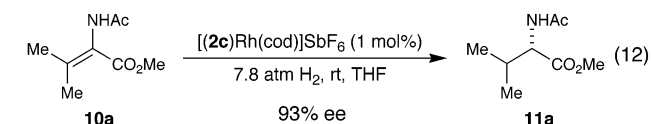
R	P	% ee <sup>b,d</sup> (S)	% ee <sup>b,e</sup> (R)
Me	Ac ( <b>6a</b> )	97	97
H	Ac ( <b>8a</b> )	96	97
Me	Bz ( <b>8b-Z</b> )	94	90
Me	Bz ( <b>8b-E</b> )	94	87
Me	Cbz ( <b>8c</b> )	95	94 (80% conv)
Me	Boc ( <b>8d</b> )	95	83

<sup>a</sup> All reactions proceeded to complete conversion, except where noted otherwise. <sup>b</sup> Absolute stereochemistry of the products determined by correlation of optical rotations to literature values. <sup>c</sup> Enantiomeric excess determined by chiral GC (Chirasil L-Val). <sup>d</sup> 7.8 atm H<sub>2</sub>. <sup>e</sup> 1 atm H<sub>2</sub>.

with ligand **2c**. Furthermore, deuteration of the two olefin isomers afforded two diastereomeric products, indicating that olefin isomerization does not occur under the reaction conditions (eqs 10,11).<sup>15</sup> The free acid can also be hydrogenated with the same selectivity as the methyl ester.



Hydrogenation of tetrasubstituted enamides is particularly challenging for most Rh hydrogenation catalysts.<sup>16</sup> Ligand **2c** was effective in the hydrogenation of  $\beta,\beta$ -disubstituted aceta-midoacrylates **10a,b** affording products **11a,b** in high enantioselectivity (eqs 12,13). Aryl enamides **12a,b** were also good

**Figure 3.** Standard Rh-catalyzed hydrogenation mechanism.

substrates for hydrogenation using this ligand, affording the protected chiral amines **13a,b** in >90% ee (eqs 14,15).<sup>17</sup>

**Mechanistic Observations.** The mechanism of the Rh-catalyzed hydrogenation has been extensively studied.<sup>18</sup> Most catalysts operate via the mechanism depicted in Figure 3.<sup>19</sup> Initial formation of a bidentate catalyst–substrate complex is followed by oxidative addition of hydrogen, migratory insertion to form an alkyl hydride, and reductive elimination to regenerate the unsaturated rhodium complex. The oxidative addition step is known to be rate-determining in almost all cases.<sup>20</sup> A few examples of substrate–catalyst complexes in these reduction processes have been isolated and structurally characterized by NMR spectroscopy<sup>18,21</sup> or X-ray crystallography,<sup>22</sup> and in every case, hydrogenation of the major diastereomer of the complex predicts the wrong stereochemistry of the product. Addition of dihydrogen to the minor, and sometimes unobserved, diastereomer is more rapid and leads to the observed sense of induction. The decrease in enantioselectivity with increasing hydrogen pressure is a direct result of this Curtin–Hammett-type situation, although the absence of such an effect does not necessarily imply that the reaction is proceeding through the major diastereomer.<sup>21b</sup>

The solid-state structure of Rh complex **14**<sup>23</sup> reinforces the salient features observed in the Pd and Rh structures in Figure 1 and provides further evidence that this is a general trend

- (15) Koenig, K.; Knowles, W. *J. Am. Chem. Soc.* **1978**, *100*, 7561–7564.  
 (16) (a) Burk, M. J.; Gross, M. F.; Martinez, J. P. *J. Am. Chem. Soc.* **1995**, *117*, 9375–9376. (b) Imamoto, T.; Watanabe, J.; Wada, Y.; Masuda, H.; Yamada, H.; Tsuruta, H.; Matsukawa, S.; Yamaguchi, K. *J. Am. Chem. Soc.* **1998**, *120*, 1635–1636.  
 (17) (a) Burk, M. J.; Wang, Y. M.; Lee, J. R. *J. Am. Chem. Soc.* **1996**, *118*, 5142–5143. (b) Zhu, G.; Zhang, X. *J. Org. Chem.* **1998**, *63*, 9590–9593. (c) Xiao, D.; Zhang, Z.; Zhang, X. *Org. Lett.* **1999**, *1*, 1679–1682. (d) Yan, Y.-Y.; RajanBabu, T. V. *Org. Lett.* **2000**, *2*, 4137–4140.  
 (18) Gridnev, I. D.; Higashi, N.; Asakura, K.; Imamoto, T. *J. Am. Chem. Soc.* **2000**, *122*, 7183–7194 and references therein.  
 (19) (a) Halpern, J. *Science* **1982**, *217*, 401–407. (b) Landis, C. R.; Halpern, J. *J. Am. Chem. Soc.* **1987**, *109*, 1746–1754. (c) Brown, J. M.; Chaloner, P. *J. Am. Chem. Soc.* **1980**, *102*, 3040–3048.  
 (20) For an example where the rate-determining step appears to be migratory insertion, see ref 18.  
 (21) (a) Allen, D. G.; Wild, B.; Wood, D. L. *Organometallics* **1986**, *5*, 1009–1015. (b) Armstrong, S. M.; Brown, J. M.; Burk, M. J. *Tetrahedron Lett.* **1993**, *34*, 879–882.  
 (22) (a) Chan, A. S. C.; Pluth, J. J.; Halpern, J. *Inorg. Chim. Acta* **1979**, *37*, L477–L479. (b) Chan, A. S. C.; Pluth, J. J.; Halpern, J. *J. Am. Chem. Soc.* **1980**, *102*, 5952–5954. (c) McCulloch, B.; Halpern, J.; Thompson, M. R.; Landis, C. R. *Organometallics* **1990**, *9*, 1392–1395.  
 (23) Crystals of **14** (C<sub>33</sub>H<sub>49</sub>F<sub>6</sub>O<sub>2</sub>PRhSb) were grown by slow diffusion of Et<sub>2</sub>O into a solution of **14** in CH<sub>2</sub>Cl<sub>2</sub> to yield orange prisms. The compound crystallizes in the tetragonal crystal system, space group P4<sub>1</sub>; a = b = 10.22450(10) Å, c = 36.2454(6) Å,  $\alpha = \beta = \gamma = 90^\circ$ ; V = 3789.11(8) Å<sup>3</sup>; Z = 4; R = 0.0802, GooF = 1.219.

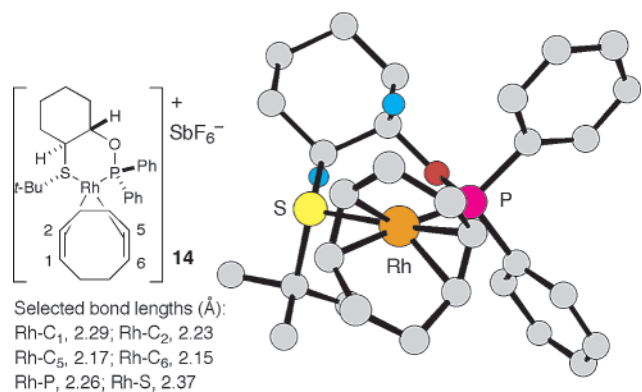


**Figure 4.** X-ray crystal structure of [(3)Rh(cod)]SbF<sub>6</sub>. Counterion omitted for clarity.

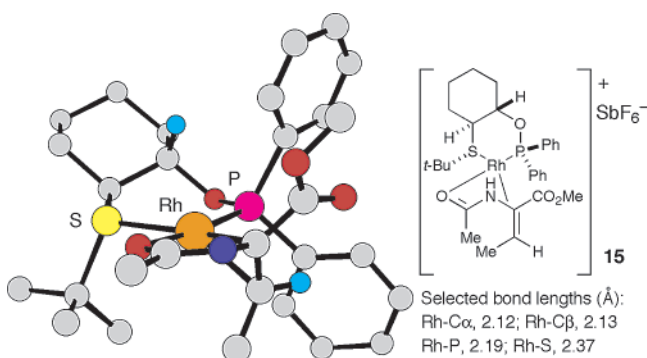
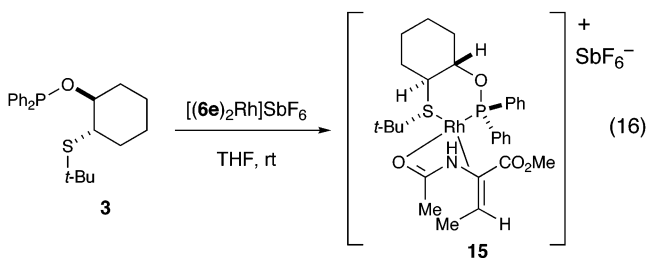


**Figure 5.** X-ray crystal structure of [(3)Rh(6e)]SbF<sub>6</sub>. Counterion omitted for clarity.

(Figure 4). Even though the substituent adjacent to the sulfur atom is smaller in **14** (primary vs secondary alkyl group), the *tert*-butyl group is still effectively geared away from the backbone of the cyclohexyl ring. This gearing may be due to the preference for the sulfur substituent to adopt a pseudoaxial position in P/S chelate rings. The steric bulk of the pseudoaxial *tert*-butyl group forces the pseudoaxial *P*-phenyl group into an edge-on conformation, allowing the pseudoequatorial *P*-phenyl group to adopt a face-on orientation. The large differences in the Rh–carbon bond distances trans to them ( $\sim 0.1$  Å) once again illustrate the difference in trans influence between the phosphinite and thioether donors.



Catalyst–substrate complex **15** was formed by reaction of [(6e)<sub>2</sub>Rh]SbF<sub>6</sub> with ligand **3** (eq 16). Remarkably, only one of the four possible diastereomers was observed in solution, as evidenced by a single set of resonances in the <sup>1</sup>H and <sup>31</sup>P NMR spectra that do not change upon cooling. Crystals of **15** were grown, and X-ray crystallographic analysis revealed the structure of the preferred isomer (Figure 5).<sup>24</sup> To understand why this isomer is favored it is helpful to consider the quadrant diagram, a model used in the analysis of other hydrogenation reactions

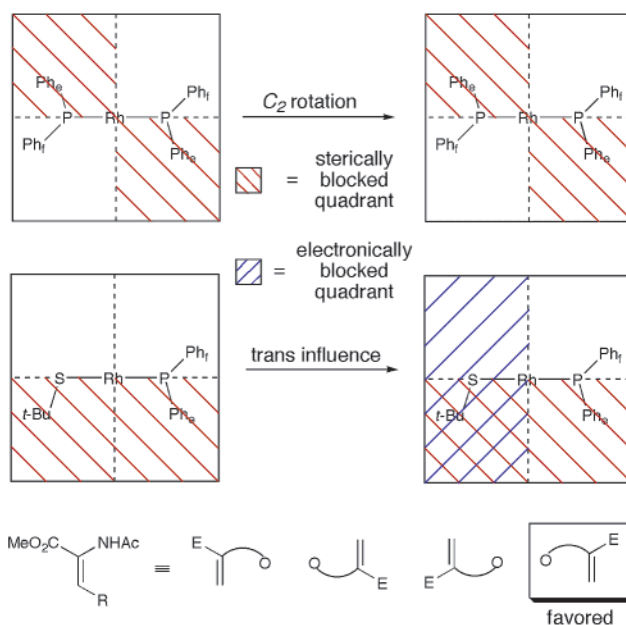


**Figure 6.** Quadrant diagrams and possible substrate orientations for C<sub>2</sub>-symmetric bisphosphines vs mixed donor ligands.

(Figure 6).<sup>2b,d,25</sup> For normal C<sub>2</sub>-symmetric bisphosphines, the edge-on/face-on alternation of the *P*-aryl groups induced by the chiral backbone blocks two diagonally disposed quadrants of the available coordination space. Furthermore, because of the native symmetry of the system, the two remaining quadrants are equivalent, and selective binding of the substrate occurs. The P/S ligand system presents a different mechanism for substrate facial discrimination. Sterically, the bulky sulfur substituent and its adjacent edge-on *P*-phenyl group block the lower left and lower right quadrants, respectively. Because of the lack of symmetry, two inequivalent sterically unencumbered quadrants are still available. These two quadrants are distinguished electronically by the trans influence. In general, ligands with stronger trans influences prefer to be coordinated opposite those with weaker trans influences.<sup>26</sup> In this structure, the olefin has the stronger trans influence of the two substrate donors, so that it prefers to be trans to the thioether. This eliminates the two left-hand quadrants, leaving only the upper right-hand quadrant open. Binding of the substrate so that the carbomethoxy group occupies this quadrant gives the observed structure of **15**. Surprisingly, addition of dihydrogen to the complexed face of the olefin in **15** explains the observed sense of induction. To our knowledge, this is the only example of X-ray crystallographic determination of a catalyst–substrate complex that correctly predicts the stereochemistry of the product.<sup>27</sup>

**Dihydrogen Addition.** Little information about the oxidative addition of dihydrogen could be obtained from Rh complexes

(24) Crystals of **15** (C<sub>33</sub>H<sub>48</sub>F<sub>6</sub>NO<sub>5</sub>PRhSb) were grown by slow diffusion of Et<sub>2</sub>O into a solution of **15** in THF to yield orange prisms. The compound crystallizes in the monoclinic crystal system, space group P2<sub>1</sub>; *a* = 10.5355(2) Å, *b* = 14.0685(2) Å, *c* = 13.7558(3) Å,  $\alpha = \gamma = 90^\circ$ ,  $\beta = 108.3525^\circ$ ; *V* = 1935.16(6) Å<sup>3</sup>; *Z* = 2; *R* = 0.0369, *Goof* = 1.026.

(25) There has been some confusion because the quadrant diagram has been used both to correlate the catalyst structure with the product stereochemistry and also to predict or explain the structure of the catalyst–substrate complex (often incorrectly). Here we use it for the latter purpose. (a) Knowles, W. S. *Acc. Chem. Res.* **1983**, *16*, 106–112. (b) Komarov, I. V.; Börner, A. *Angew. Chem., Int. Ed.* **2001**, *40*, 1197–1200.

(26) The enthalpy of the isomerization of *trans*-(Et<sub>3</sub>P)<sub>2</sub>PtCl<sub>2</sub> to the *cis* isomer is  $-2.5$  kcal/mol, despite the greater steric interaction in the latter. See Chatt, J.; Wilkins, R. G. *J. Chem. Soc.* **1952**, 4300–4306.

of the P/S ligands. Under a variety of hydrogenation conditions, with many different Rh complexes, no hydridorhodium(III) species were isolated or observed. In many cases where Rh complexes fail to give stable oxidative addition products, use of the corresponding iridium complexes allows their observation or isolation due to the higher propensity for iridium to undergo oxidative addition and its corresponding reluctance to reductively eliminate.<sup>28</sup> Accordingly, iridium(I) complex **16** was prepared to take advantage of this property to study the oxidative addition step. The X-ray crystal structure of iridium complex **16** (Figure 8)<sup>29</sup> is nearly identical to that of its Rh congener **14**.

The electronic<sup>30</sup> and steric<sup>31</sup> effects on the kinetic selectivity of dihydrogen addition to other iridium complexes have been previously reported. The four potential cis-dihydride addition products of **16** are illustrated schematically in Figure 7. If dihydrogen addition occurs along the axis of the phosphinite, isomers A and C would be produced; if addition is parallel to the thioether, B and D would predominate. Furthermore, addition of dihydrogen may occur either to the top face of the iridium complex (opposite the *S*-*tert*-butyl substituent) to give A or B, or to the bottom face to give C or D. Upon treatment of iridium complex **16** with H<sub>2</sub> for 1 min at -78 °C, complete conversion to a dihydride complex **17** was observed. Remarkably, only one diastereomer of this dihydride is visible in the <sup>1</sup>H and <sup>31</sup>P NMR spectra. The relatively low chemical shifts ( $\delta$  -13.0 and -14.1 ppm) and small phosphorus-hydride coupling constants ( $J$  = 20, 22 Hz) of the hydrides indicate that they are both cis to the phosphorus donor.<sup>31,32</sup> Only structures B and D satisfy that condition, both of which are the product of addition parallel to the sulfur donor, but these possibilities could not be distinguished by NMR spectroscopy.

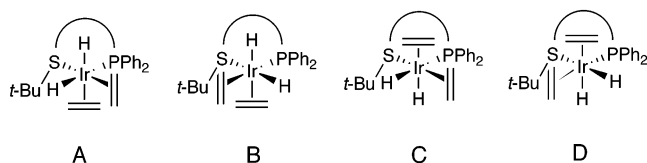


Figure 7. Possible kinetic products of dihydrogen addition to **16**.

No change in the composition of the dihydride was observed upon warming to room temperature, indicating that the thermodynamic oxidative addition product is the same as the kinetic adduct. Crystals of [(3)Ir(cod)H<sub>2</sub>]SbF<sub>6</sub> (**17**) were obtained and analyzed by X-ray crystallography (Figure 8).<sup>33</sup> This structure corresponds to isomer D in Figure 5. In keeping with the dictates

of the trans influence, the three strongest donors (H, H, and P) are trans to the three weakest donors (olefin, S, and olefin, respectively). The trans influence is also manifested in the increased bond lengths of the olefin and sulfur donors trans to hydride compared to those in the iridium(I) structure **16**. Interestingly, this isomer is a result of addition of dihydrogen to the more sterically encumbered face of the complex (i.e., syn to the *tert*-butyl group).<sup>34</sup> Addition to the opposite face would result in strong steric interaction between the migrating olefin substituent and the pseudoaxial *tert*-butyl and phenyl groups in both the trigonal bipyramidal intermediate and the addition product, and this may be the reason it is not observed.

A possible explanation for the difference in the rate of addition of dihydrogen to the catalyst–substrate complexes is illustrated in Figure 9.<sup>35</sup> Assuming the selectivity of the oxidative addition of dihydrogen is the same for the catalyst–substrate complex **15** as it is for the cyclooctadiene iridium complex **16** (i.e. parallel to the thioether and from the face syn to the *S*-*tert*-butyl group),<sup>36</sup> addition of dihydrogen to the major catalyst–substrate complex **15**-maj would give dihydride complex **18**. This isomer is stereoelectronically aligned to undergo migratory insertion to form the alkylhydride complex **19**. On the other hand, similar oxidative addition to the minor diastereomer would afford dihydride complex **20**, which is not properly aligned to undergo migratory insertion. Either significant rearrangement of this intermediate or addition of dihydrogen via one of the unfavored pathways would be required to produce the alkylhydride intermediate and continue the catalytic cycle. The putative difference in migration rates may be responsible for the faster reaction of the major catalyst–substrate diastereomer and the unique mechanism exhibited by this catalyst.

## Hydrosilylation of Ketones

**Catalyst Optimization.** Given the success of this ligand class in the hydrogenation reaction, it seemed likely that other enantioselective Rh-catalyzed processes might be realized with this ligand family. As an example, we chose the asymmetric hydrosilylation of ketones. While a variety of ligand classes have been used for this reaction, application of mixed P/S ligands has met with little success.<sup>37</sup> Preliminary ligand screening in the reduction of acetophenone with diphenylsilane showed that Rh complex **14** derived from ligand **3** resulted in moderately high enantioselectivity (Table 4) with less than 5% enolsilane formation by <sup>1</sup>H NMR spectroscopic analysis. All other catalysts gave poorer results.

- (27) This has recently been claimed to be true for a bisphosphetane ligand on the basis of circumstantial evidence, but no structural data has been presented to bolster this claim. See Marinetti, A.; Jus, S.; Genet, J.-P. *Tetrahedron Lett.* **1999**, *40*, 8365–8368. Some skepticism has been expressed as to their conclusions, see footnote 21 in Landis, C. R.; Feldgus, S. *Angew. Chem., Int. Ed.* **2000**, *39*, 2863–2866
- (28) Crabtree, R. H. *The Organometallic Chemistry of the Transition Metals*, 2nd ed.; Wiley-Interscience: New York, 1994.
- (29) Crystals of **16** (C<sub>30</sub>H<sub>41</sub>F<sub>6</sub>IrOPSSb+C<sub>4</sub>H<sub>10</sub>O) were grown by slow diffusion of Et<sub>2</sub>O into a solution of **16** in CH<sub>2</sub>Cl<sub>2</sub> to yield red prisms. The compound crystallizes in the tetragonal crystal system, space group P4<sub>1</sub>;  $a = b = 10.2022(8)$  Å,  $c = 36.270(4)$  Å,  $\alpha = \beta = \gamma = 90^\circ$ ;  $V = 3775.2(6)$  Å<sup>3</sup>;  $Z = 5$ ;  $R = 0.0310$ ,  $\text{Goof} = 1.032$ .
- (30) (a) Burk, M. J.; McGrath, M. P.; Wheeler, R.; Crabtree, R. H. *J. Am. Chem. Soc.* **1988**, *110*, 5034–5039. (b) Deutsch, P. P.; Eisenberg, R. *Chem. Rev.* **1988**, *88*, 1147–1161.
- (31) (a) Halg, W. J.; Ohrstrom, L. R.; Ruegger, H.; Venanzi, L. M. *Magn. Reson.* **1993**, *31*, 677–684. (b) Kimmich, B. F. M.; Somsok, E.; Landis, C. R. *J. Am. Chem. Soc.* **1998**, *120*, 10115–10125.
- (32) Hydrides trans to the phosphorus donor generally have coupling constants of 80–100 Hz. See ref 31.

- (33) Crystals of **17** (C<sub>30</sub>H<sub>43</sub>F<sub>6</sub>IrOPSSb) were grown by slow diffusion of Et<sub>2</sub>O into a solution of **17** in CH<sub>2</sub>Cl<sub>2</sub> to yield colorless needles. The compound crystallizes in the monoclinic crystal system, space group P2<sub>1</sub>;  $a = 10.4130(16)$  Å,  $b = 11.5788(18)$  Å,  $c = 13.786(2)$  Å,  $\alpha = \gamma = 90^\circ$ ,  $\beta = 96.320(3)^\circ$ ;  $V = 1652.1(5)$  Å<sup>3</sup>;  $Z = 2$ ;  $R = 0.0314$ ,  $\text{Goof} = 1.034$ .
- (34) Although diastereomeric equilibration is not impossible, previous studies of iridium dihydrides have shown that isomerization only occurs above -50 °C, see refs 30, 31.
- (35) We cannot eliminate the possibility that it is simply the predominance of the observed isomer, rather than its faster rate of reaction, that is responsible for the enantioselectivity.
- (36) Note that the native selectivities of the P/S ligand and the substrate are reinforcing in these complexes, that is, the former prefers addition parallel to the thioether, and the latter prefers addition parallel to the olefin. See: Brown, J. M.; Maddox, J. J. *J. Chem. Soc., Chem. Commun.* **1987**, 1278–1280.
- (37) For other mixed P/S ligands in asymmetric hydrosilylation, see: (a) Hiraoka, M.; Nishikawa, A.; Morimoto, T.; Achiwa, K. *Chem. Pharm. Bull.* **1998**, *46*, 704–706. (b) Nishibayashi, Y.; Segawa, K.; Singh, J. D.; Fukuzawa, S.; Ohe, K.; Uemura, S. *Organometallics* **1996**, *15*, 370–379.

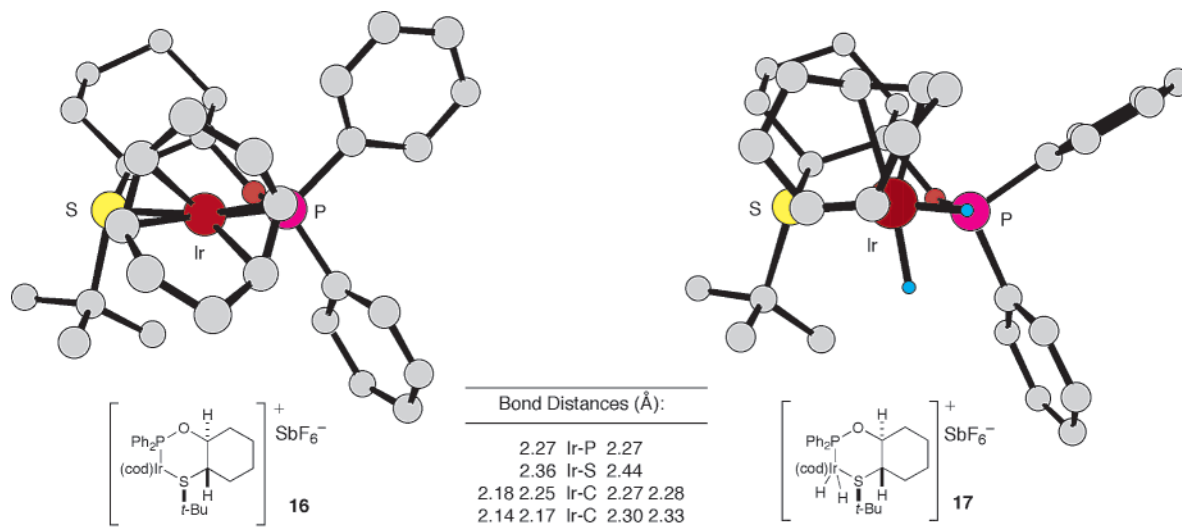
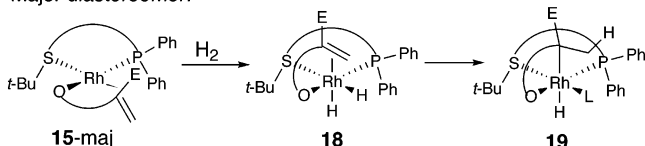


**Figure 8.** X-ray crystal structures of **16** and **17**. Counterions omitted for clarity. The positions of the hydrides in **17** were calculated.

Major diastereomer:



Minor diastereomer:

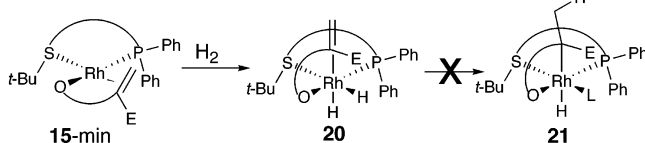


**Figure 9.** Rationalization of the relative rates of addition of dihydrogen to substrate–catalyst complexes.

**Table 4.** Hydrosilylation of Acetophenone with Mixed Phosphorus/Sulfur Ligands (eq 17)

Ph-C(=O)-Me + Ph <sub>2</sub> SiH <sub>2</sub> <sup>a</sup>		1 mol% [(L*)Rh(cod)]SbF <sub>6</sub>	H <sub>3</sub> O <sup>+</sup>	Ph-CH(OH)-Me	(17)
22a	23c	THF, rt		24a	
L*				% ee <sup>b</sup> (% yield)	
<b>1a</b>				-62 (36)	
<b>2a</b>				-51 (89)	
<b>2b</b>				20 (50)	
<b>3</b>				86 (90)	

<sup>a</sup> 1.5 equiv of silane were used. <sup>b</sup> Determined by chiral GC (Cyclodex B). Configuration assigned by comparison of optical rotation to literature values.

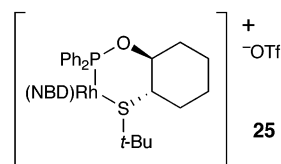
Reactions employing Rh complexes bearing a cyclooctadiene ligand and a hexafluoroantimonate counterion led to large amounts of oxidative silane coupling products, often accompanied by vigorous hydrogen evolution and uncontrollable reaction exotherms.<sup>38</sup> Lowering the reaction temperature in an effort to control the exotherm reduced the enantioselectivity. After an extensive screen of Rh sources, it was found that complex **25**, with a norbornadiene ligand and a triflate counterion, ameliorated this problem. Use of this catalyst complex resulted in increased selectivity for ketone reduction, smaller

**Table 5.** Effect of Silane Structure on the Hydrosilylation of Acetophenone with Mixed Phosphorus/Sulfur Ligands (eq 18)<sup>a</sup>

Ph-C(=O)-Me + Silane	1 mol% <b>25</b>	H <sub>3</sub> O <sup>+</sup>	Ph-CH(OH)-Me	(18)
22a	23a-g	THF, rt	24a	
silane <sup>a</sup>				% ee <sup>b</sup>
PhSiH <sub>3</sub> ( <b>23a</b> )				0
PhMeSiH <sub>2</sub> ( <b>23b</b> )				78
Ph <sub>2</sub> SiH <sub>2</sub> ( <b>23c</b> )				88
Ph(1-naphthyl)SiH <sub>2</sub> ( <b>23d</b> )				95
Ph( <i>t</i> -Bu)SiH <sub>2</sub> ( <b>23e</b> )				NR
Et <sub>3</sub> SiH ( <b>23f</b> )				NR
PMHS ( <b>23g</b> )				NR

<sup>a</sup> 1.5 equiv of silane were used. <sup>b</sup> Determined by chiral GC analysis (Cyclodex B).

amounts of silane polymerization, and even a slight increase in enantioselectivity.



Further optimization of the catalytic system led us to explore the influence of the silane structure on the enantioselectivity of this reduction (Table 5). While diphenylsilane is the standard stoichiometric reducing agent in most Rh-catalyzed hydrosilylations, we found that the size of the silane reductant had a major effect on the selectivity and reactivity of the hydrosilylation. Diphenylsilane, using catalyst **25**, reduced acetophenone in under 5 min at room temperature to give **24a** in 88% ee. When one of the phenyl substituents on the silane was replaced by a smaller substituent such as methyl, **23b**, or hydrogen, **23a**, the enantioselectivity decreased to 78 and 0% ee, respectively. On the other hand, increasing the size of that substituent to 1-naphthyl, **23d**, increased the enantioselectivity to 95% ee.<sup>39</sup> Any additional increase in the size of the silane shut down all

(38) For references on silane polymerization mechanisms, see: (a) Tilley, T. D.; Woo, H. G. *Polym. Prepr. Am. Chem. Soc., Div. Polym. Chem.* **1990**, *31*, 228–289. (b) Tilley, T. D. *Comments Inorg. Chem.* **1990**, *10*, 37–51.

(39) (a) Ojima, I.; Kogure, T.; Kumagai, M. *J. Org. Chem.* **1977**, *42*, 1671–1679. (b) Balavoine, G.; Clinet, J. C.; Lellouche, T. *Tetrahedron Lett.* **1989**, *30*, 5141–5144.



**Table 6.** Asymmetric Hydrosilylation of Aryl Methyl Ketones with Mixed Phosphorus/Sulfur Ligands (eq 19)

Ar	% ee <sup>a</sup> (% yield)
Ph ( <b>24a</b> )	95 (80) <sup>b,c</sup>
2-MePh ( <b>24b</b> )	95 (98) <sup>c</sup>
4-MePh ( <b>24c</b> )	92 (90) <sup>c</sup>
2-MeOPh ( <b>24d</b> )	95 (90) <sup>d</sup>
4-MeOPh ( <b>24e</b> )	88 (56) <sup>d,f</sup>
2-ClPh ( <b>24f</b> )	98 (90) <sup>d</sup>
4-ClPh ( <b>24g</b> )	85 (95) <sup>c</sup>
1-naphthyl ( <b>24h</b> )	98 (99) <sup>e</sup>
2-naphthyl ( <b>24i</b> )	95 (99) <sup>e</sup>

<sup>a</sup> 1.5 equiv of silane were used. <sup>b</sup> At 23 °C. <sup>c</sup> Determined by chiral GC (Cyclodex B). <sup>d</sup> Determined by chiral HPLC (Daicel Chiralcel OB). <sup>e</sup> Determined by chiral HPLC (Daicel Chiralcel OJ). <sup>f</sup> Using 0.011 equiv of **3** and 0.005 equiv of [Rh(NBD)Cl]<sub>2</sub>. <sup>g</sup> Absolute configuration was assigned by comparison of optical rotations to literature values.

**Table 7.** Asymmetric Hydrosilylation of Phenyl Alkyl Ketones with Mixed Phosphorus/Sulfur Ligands (eq 20)

R	% ee <sup>a</sup> (% yield)
Me ( <b>24a</b> )	95 (80) <sup>b,c</sup>
Et ( <b>24j</b> )	94 (95) <sup>c</sup>
<i>i</i> -Bu ( <b>24k</b> )	94 (95) <sup>c</sup>
Bn ( <b>24l</b> )	94 (75) <sup>d</sup>

<sup>a</sup> 1.5 equiv of silane were used. <sup>b</sup> At 23 °C. <sup>c</sup> Determined by chiral GC (Cyclodex B). <sup>d</sup> Determined by chiral HPLC (Daicel Chiralcel OB).

reaction, and tertiary silanes also showed no reactivity. Phenyl-(1-naphthyl)silane is easily prepared from 1-naphthyl bromide and PhSiCl<sub>3</sub> in a one-pot procedure in 90% yield.<sup>40</sup>

**Hydrosilylation of Aromatic Ketones.** Catalyst **25** was found to afford high enantioselectivities in the reduction of a variety of aryl methyl ketones (Table 6). The increased reactivity of this catalyst allowed the hydrosilylations to be run at lower temperatures, generally resulting in higher selectivity. Interestingly, the only exception is in the case of acetophenone (95% ee at room temperature vs 91% ee at -20 °C).<sup>41</sup> We found that ortho substitution resulted in higher selectivities in the hydrosilylation (**22b,d,f,h**), while para substitution gave lower selectivities (**22c,e,g**). *p*-Methoxyacetophenone (**22e**) was completely consumed in the reaction, however, it gave only non-hydrolyzable silicon-containing products upon quenching.<sup>42</sup> In this case, the less reactive chloride catalyst could be used to deliver the desired alcohol in 56% yield and 88% ee. A variety of phenyl alkyl ketones could also be hydrosilylated in high selectivity and yield (Table 7).

Cyclic aromatic ketones were also reduced in moderate-to-high enantioselectivities (Table 8). Increasing ring size was found to be favorable for high enantioselectivities as exemplified by the benzosuberone reduction (98% ee). It is particularly noteworthy that in the case of thiochromanone (**27d**), the

**Table 8.** Asymmetric Hydrosilylation of Cyclic Aryl Alkyl Ketones with Mixed Phosphorus/Sulfur Ligands (eq 21)

Alcohol <sup>d</sup>	% ee (% yield)
( <b>27a</b> )	85 <sup>b</sup> (90)
( <b>27b</b> ) X = CH <sub>2</sub> , ( <b>27b</b> )	91 <sup>b</sup> (90)
( <b>27c</b> ) X = O, ( <b>27c</b> )	95 <sup>b</sup> (90)
( <b>27d</b> ) X = S, ( <b>27d</b> )	92 <sup>b</sup> (91)
( <b>27e</b> )	98 <sup>c</sup> (90)

<sup>a</sup> 1.5 equiv of silane were used. <sup>b</sup> Determined by chiral HPLC (Daicel Chiralcel OB). <sup>c</sup> Determined by chiral GC (Cyclodex B). <sup>d</sup> Absolute configuration assigned by comparison of optical rotations to literature values.

reaction still proceeded with high selectivity and yield, despite the presence of a potentially confounding (and coordinating) thioether in the substrate.

**Hydrosilylation of Dialkyl Ketones.** Nonaromatic ketones showed similar reactivities and selectivities in the hydrosilylation (Table 9).<sup>43</sup> 1-Acetylcyclohexene was reduced cleanly using the chloride catalyst to give the allylic alcohol with less than 5% conjugate reduction as determined by <sup>1</sup>H NMR. The slightly lower yields in the reduction of pinacolone and 1-acetylcyclohexene are due to the volatility of the products.

$\beta$ -Ketoesters could also be reduced in high selectivity with this catalyst, provided there was sufficient steric differentiation between the two carbonyl substituents (Table 10).<sup>44</sup> Alcohol **31b** could be produced in excellent enantioselectivity and good yield on a 12-g scale, highlighting the utility of this process. The monosubstituted ketoester **30c** afforded a 1:1 mixture of diastereomers each in 98% ee. Unfortunately, unsubstituted  $\beta$ - and  $\alpha$ -ketoesters did not give good levels of enantioselectivity.

The mechanism and stereochemical rationale for the Rh-catalyzed asymmetric hydrosilylation are not well understood. In this system, the enantioselectivity appears to be dictated purely by steric effects. The stereochemistry of the products can be predicted on the basis of an analysis of the relative size of the two ketone substituents. Specifically, with the larger ketone substituent oriented to the left, attack from the bottom face of the ketone gives the observed stereoselection.

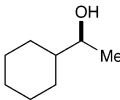
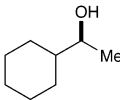
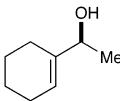
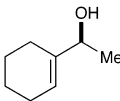
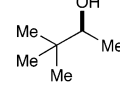
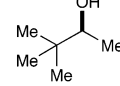
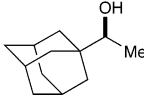
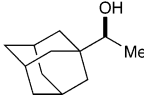
(42) For other catalysts that display unusual reactivity patterns with *p*-methoxyacetophenone, see: Lee, S.-G.; Lim, C. W.; Song, C. E.; Kim, I. O. *Tetrahedron: Asymmetry* **1997**, *8*, 4027–4031. Nishibayashi, Y.; Singh, J. D.; Segawa, K.; Fukuzawa, S.; Uemura, S. *J. Chem. Soc., Chem. Commun.* **1994**, 1375–1376.

(43) For other hydrosilylation catalysts displaying high enantioselectivity with alkyl ketones, see: Sawamura, M.; Kuwano, R.; Ito, Y. *Angew. Chem., Int. Ed. Engl.* **1994**, *33*, 111–113. Nishibayashi, Y.; Segawa, K.; Ohe, K.; Uemura, S. *Organometallics* **1995**, *14*, 5486–5487.

(44) For other enantioselective ketoester hydrosilylations, see: ref 39a and (a) Nishiyama, H.; Sakaguchi, H.; Nakamura, T.; Horihata, M.; Kondo, M.; Itoh, K. *Organometallics* **1989**, *8*, 846–848. (b) Nishiyama, H.; Kondo, M.; Nakamura, T.; Itoh, K. *Organometallics* **1991**, *10*, 500–508. (c) Kuwano, R.; Sawamura, M.; Shirai, J.; Takahashi, M.; Ito, Y. *Tetrahedron Lett.* **1995**, *36*, 5239–5242.

(40) Corriu, R.; Lanneau, G.; Royo, G. *Bull. Soc. Chim. Fr.* **1968**, 458–459.  
(41) For other hydrosilylation catalysts that display unusual temperature profiles, see: ref 39a and (a) Enders, D.; Gielen, H.; Breuer, K. *Tetrahedron: Asymmetry* **1997**, *8*, 3571–3574. (b) Haag, D.; Runsink, J.; Scharf, H.-D. *Organometallics* **1998**, *17*, 398–409.

**Table 9.** Asymmetric Hydrosilylation of Dialkyl Ketones with Mixed Phosphorus/Sulfur Ligands (eq 22)

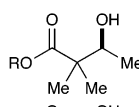
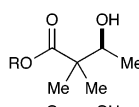
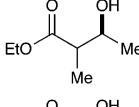
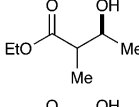
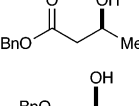
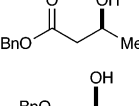
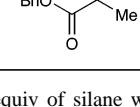
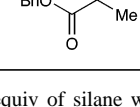
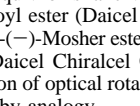
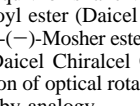
Ketone + Ph(1-Naphthyl)SiH <sub>2</sub> <sup>a</sup>		$\xrightarrow[THF, -20\text{ }^{\circ}C]{1\text{ mol\% } \mathbf{25}}$	$\xrightarrow{H_3O^+}$	Alcohol	(22)
<b>28a-d</b>	<b>23d</b>			<b>29a-d</b>	
				Alcohol	% ee <sup>b</sup> (% yield)
				 ( <b>29a</b> )	92 (90) <sup>c</sup>
				 ( <b>29b</b> )	91 (85) <sup>c,e</sup>
				 ( <b>29c</b> )	98 (75) <sup>d</sup>
				 ( <b>29d</b> )	>99 (98) <sup>c</sup>

<sup>a</sup> 1.5 equiv of silane were used. <sup>b</sup> Determined by chiral HPLC on the 1-naphthoyl ester (Daicel Chiralcel OD-H). <sup>c</sup> Absolute configuration assigned by comparison of optical rotations to literature values. <sup>d</sup> Absolute configuration assigned by analogy. <sup>e</sup> Using 0.011 equiv of **3** and 0.005 equiv of [(NBD)RhCl]<sub>2</sub>.

## Conclusions

We have successfully extended the use of chiral mixed phosphorus/sulfur ligands **1–3** to two Rh-catalyzed processes, namely, the hydrogenation of olefins and the hydrosilylation of size-differentiated ketones. Both processes are effective with a wide variety of substrates, giving high levels of enantioselectivity. The model proposed for the hydrogenation involves regioselective binding of the substrate determined by the difference in trans influence between the phosphorus and sulfur donors and enantiofacial discrimination based on the gearing of the *P*-phenyl groups induced by the newly formed sulfur stereocenter. Furthermore, a similar combination of steric and electronic effects is responsible for high selectivity in the oxidative addition step. In both steps, the ligand exerts a

**Table 10.** Asymmetric Hydrosilylation of Cyclic Ketoesters with Mixed Phosphorus/Sulfur Ligands (eq 23)

Ketone + Ph(1-Naphthyl)SiH <sub>2</sub> <sup>a</sup>		$\xrightarrow[THF, -20\text{ }^{\circ}C]{1\text{ mol\% } \mathbf{25}}$	$\xrightarrow{H_3O^+}$	Alcohol	(23)
<b>30a-e</b>	<b>23d</b>			<b>31a-e</b>	
				Alcohol	% ee (% yield)
				 ( <b>31a</b> )	99 <sup>b,e</sup> (94)
				 ( <b>31b</b> )	>99 <sup>b,e</sup> (80)
				 ( <b>31c</b> )	1:1 syn:anti 98 <sup>b,f</sup> (80)
				 ( <b>31d</b> )	40 <sup>d,f</sup> (70)
				 ( <b>31e</b> )	46 <sup>d,f</sup> (92)

<sup>a</sup> 1.5 equiv of silane were used. <sup>b</sup> Determined by chiral HPLC on the 1-naphthoyl ester (Daicel Chiralcel OD-H). <sup>c</sup> Determined by chiral HPLC on the (*S*)-(-)-Mosher ester (Daicel Chiralcel OD-H). <sup>d</sup> Determined by chiral HPLC (Daicel Chiralcel OD-H). <sup>e</sup> Absolute configuration determined by comparison of optical rotations to literature values. <sup>f</sup> Absolute configuration assigned by analogy.

remarkable level of selectivity, selecting only one of four possible diastereomers. Overall, this process constitutes the first documented example in which the preferred diastereomer of the catalyst–substrate complex leads to the observed stereochemistry of the product.

**Acknowledgment.** Support has been provided by the NIH (GM18595), the NSF, and Merck. The NIH BRS Shared Instrumentation Grant Program 1-S10-RR04870 and the NSF (CHE 88-14019) are acknowledged for providing NMR facilities.

**Supporting Information Available:** Complete experimental procedures, characterization of new compounds, and X-ray structure data (PDF). This material is available free of charge via the Internet at <http://pubs.acs.org>.

JA012639O